

# Dilatometric analysis of phase transformations in hypo-eutectoid steels

T. A. KOP, J. SIETSMA, S. VAN DER ZWAAG

*Delft University of Technology, Laboratory for Materials Science, Rotterdamseweg 137, 2628 AL Delft, The Netherlands*

*E-mail: s.vanderzwaag@tnw.tudelft.nl*

Dilatometry is a useful technique to obtain experimental data concerning transformation kinetics in ferrous alloys. This technique is commonly used in cooling experiments to study the austenite decomposition of hypo-eutectoid steel grades. In the standard analysis of the dilatation signal there are two factors that are normally neglected. During the pro-eutectoid ferrite formation the austenite enriches in carbon, resulting in a non-linear temperature dependence of the specific austenitic volume. Furthermore, the specific volume of the formed ferrite is considerably different from that of the formed pearlite. In total not taking into account these two effects can lead to an error in the determined fraction ferrite of up to 25%. A method is presented that takes into account the two above-mentioned factors. In order to determine both the fraction ferrite and the fraction pearlite, in the analysis the temperature range of the transformation is divided into a ferrite-formation range and a pearlite-formation range. Two possible criteria for this division are discussed, and it is shown that the choice does not have an essential influence on the results. © 2001 Kluwer Academic Publishers

## 1. Introduction

The production of hot-rolled steel plates with desired mechanical properties is a very complex process. A whole range of material properties, such as good formability or high strength, can be obtained by small variations in the amounts of alloying elements or in the process parameters, such as the temperature programme and the rolling parameters. Although there is a reasonable degree of empirical knowledge concerning steel-making, the endeavour to produce superior qualities, whilst at the same time reducing costs, drives a considerable effort of fundamental research to obtain a more profound knowledge about the physical processes governing the austenite ( $\gamma$ ) to ferrite ( $\alpha$ ) phase transformation. The importance of this research arises from the fact that it is this phase transformation that determines to a considerable extent the microstructure, and thereby the properties, of the final product.

Several models exist that predict the  $\gamma \rightarrow \alpha$  transformation kinetics [1–7]. All models are developed by comparing and relating the model to experimental data. To obtain a reliable model it is therefore essential to have reliable experimental data. A technique often used to obtain information on the transformation kinetics, i.e. fractions austenite and ferrite as a function of temperature and time, is dilatometry [8, 9]. Dilatometry registers length changes that occur during the heat treatment of a sample. A common method to determine the remaining fraction austenite as a function of temperature is to extrapolate the linear expansion behaviour from the temperature regions where no

transformations occur, and to subsequently assume a proportionality between the fraction decomposed austenite and the observed length change. We will refer to this method as the lever-rule method. It should be realised, however, that this approach is valid only if a single, non-partitioning phase transformation occurs. In the case of carbon-containing alloys, this method is not applicable for two reasons [10–12]: (1) the carbon redistributes between the forming ferrite and the remaining austenite, which increases the specific volume of the austenite, and (2) the formation of pearlite has a distinctly different volume effect than the formation of ferrite. In the present paper the dilatometric effects occurring during continuous cooling of carbon-containing steels are analysed taking these effects into account. In addition the effect of two different assumptions concerning the temperature range of the pearlite formation is shown. Experiments performed on steel alloys containing 0.2–2.1 at.%C (0.05–0.45 wt.%) are used to illustrate the method.

## 2. Theory

The applicability of dilatometry in phase transformation research is due to the change of the specific volume of a sample during a phase transformation. When a material undergoes a phase change, the lattice structure changes and this is in principle accompanied by a change in specific volume. Upon cooling of a pure iron sample from temperatures above the  $A_3$  temperature, the austenite, having a face-centred cubic structure, will

transform into ferrite, having the less closely packed body-centred cubic structure. This phase transformation will cause a volume expansion of about 1.6%.

In the case of steel the iron is alloyed. The alloying gives rise to multi-phase regions in the phase diagram. When a material transforms in such a multi-phase region two processes occur. The lattice transformation takes place, but in addition there will be a redistribution of alloying elements. This means that the composition of the newly formed phase is not equal to the overall composition of the decomposing phase. Consequently, the composition of the decomposing phase changes. This gives rise to a change in the specific volume of this phase. More specifically, a sample of a hypo-eutectoid carbon steel cooled from the austenite region, will cross the austenite/ferrite two-phase region. During the transformation the austenite will gradually transform into ferrite, in which the maximum solubility of carbon is limited, and the remaining austenite will enrich in carbon. Both the formation of ferrite and the enrichment of austenite cause an expansion of the sample. This can be seen in Fig. 1. Using the expressions for the lattice parameters for Fe-C alloys [10, 13–16], see Table I, the atomic volume  $V^\gamma$  of austenite as a function of the carbon fraction,  $\xi$ , is shown at an example temperature of 900 K. It can be seen that with increasing carbon content the austenitic volume

TABLE I Lattice parameters of ferrite ( $\alpha$ ) and austenite ( $\gamma$ ) and of the orthorhombic phase cementite ( $\theta$ ) as a function of temperature  $T$  and the atomic fraction carbon ( $\xi$ ) [10, 13–16]

Phase	Lattice parameters ( $\text{\AA}$ )
$\alpha$	$a_\alpha = 2.8863 \text{\AA} (1 + 17.5 \times 10^{-6} \text{K}^{-1} [T - 800 \text{K}])$ $800 \text{K} < T < 1200 \text{K}$
$\gamma$	$a_\gamma = (3.6306 + 0.78\xi) \text{\AA} (1 + (24.9 - 50\xi)10^{-6} \text{K}^{-1} [T - 1000 \text{K}])$ $1000 \text{K} < T < 1250 \text{K}; 0.0005 < \xi < 0.0365$
$\theta$	$a_\theta = 4.5234 \text{\AA} (1 + \{5.311 \times 10^{-6} - 1.942 \times 10^{-9} \text{K}^{-1} T + 9.655 \times 10^{-12} \text{K}^{-2} T^2\} \text{K}^{-1} [T - 293 \text{K}])$ $b_\theta = 5.0883 \text{\AA} (1 + \{5.311 \times 10^{-6} - 1.942 \times 10^{-9} \text{K}^{-1} T + 9.655 \times 10^{-12} \text{K}^{-2} T^2\} \text{K}^{-1} [T - 293 \text{K}])$ $c_\theta = 6.7426 \text{\AA} (1 + \{5.311 \times 10^{-6} - 1.942 \times 10^{-9} \text{K}^{-1} T + 9.655 \times 10^{-12} \text{K}^{-2} T^2\} \text{K}^{-1} [T - 293 \text{K}])$ $300 \text{K} < T < 1000 \text{K}$

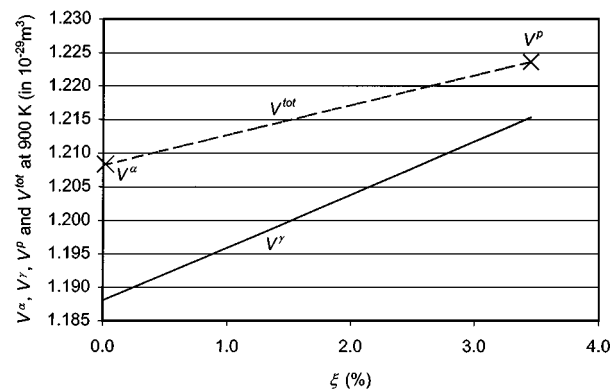


Figure 1 The atomic volumes of austenite,  $V^\gamma$ , and of a system composed of equilibrium fractions ferrite and pearlite,  $V^{\text{tot}}$ , depending on the carbon concentration at a temperature of 900 K. The atomic volumes of ferrite,  $V^\alpha$ , and pearlite,  $V^p$ , are depicted as well.

increases. The maximum solubility of carbon in ferrite is approximately 0.09 at.%. The influence of carbon on the specific volume of ferrite is therefore limited. Upon further cooling the austenite phase decomposes into the equilibrium low-temperature phases ferrite and pearlite, a mixture of ferrite and cementite ( $\text{Fe}_3\text{C}$ ).

The carbon-content dependence of the lattice parameters (Table I and Fig. 1) has important implications for the volume effect of the transformation. The first is that the total volume effect of the transformation depends on the carbon content of the alloy. The second is that the volume effect of the ferrite formation from austenite significantly differs from the volume effect of pearlite formation. The third is that the volume effect of the transformation of austenite to ferrite depends on the carbon concentration of the austenite. The fourth is that this volume effect consists of two contributions, namely the specific-volume difference between austenite and ferrite, and the increase of the austenite specific volume due to carbon enrichment.

When the dilatation during the phase transformation is to be analysed, the effects shown in Fig. 1 should be considered. The observed length change during the initial part of a measurement, due to the austenite to ferrite transformation, is the summation of two effects: the dilatation due to the lattice change and the enlargement of the remaining austenite due to carbon enrichment of this phase. The momentary dilatation effect therefore does not depend on the initial carbon concentration, but on the actual carbon concentration of the austenite, which depends on the degree of transformation.

The atomic volume of a sample is determined by the fractions of the phases present multiplied by their atomic volume, according to

$$V(T) = \sum_i f^i V^i(T), \quad (1)$$

where  $V$  is the average atomic volume of the sample,  $V^i$  is the atomic volume of phase  $i$ ,  $f^i$  is the volume fraction of phase  $i$ , and  $T$  is the temperature.  $i$  can be  $\alpha$  for ferrite,  $\gamma$  for austenite or  $p$  for pearlite. The atomic volumes are related to the lattice parameters (Table I) by  $V^\alpha = 1/2a_\alpha^3$ ,  $V^\gamma = 1/4a_\gamma^3$ ,  $V^p = (1 - \rho)V^\alpha + \rho V^\theta$ , with  $V^\theta = 1/12 a_\theta b_\theta c_\theta$ , and  $\rho$  the fraction cementite in the pearlite.

Equation 1 can be used to calculate the phase fractions from the volume change of a sample. However, the procedure is not completely straightforward, since only the length change is measured, from which data on three different phases are to be obtained.

Two intrinsic factors prevent an unambiguous determination of the phase fractions: the simultaneous formation of two phases, i.e. ferrite and pearlite, and the carbon-concentration dependence of the atomic volume of austenite. As such, the dilatometer can not distinguish between the formation of pro-eutectoid ferrite and pearlite. If the formation of ferrite and pearlite is assumed to take place in separate temperature regions, as is expected from the equilibrium phase diagram, the dilatation of a sample can be analysed in two steps. The complication of the austenitic volume being carbon-concentration dependent is solved by using literature data for the austenite lattice [14].

The subsequent stages of the dilatation analysis will now be outlined. At high temperatures, in the beginning of the austenite to ferrite transformation, there is no pearlite. The fraction ferrite is then given by

$$f^\alpha = \frac{V - V^\gamma}{V^\alpha - V^\gamma}, \quad (2)$$

which follows from Equation 1, with  $f^\alpha + f^\gamma = 1$ .

In principle this equation can be solved with  $V$  evaluated from the dilatometer measurement, and  $V^\alpha$  and  $V^\gamma$  from the literature (Table I). However, due to the carbon enrichment of the austenite, which depends on the momentary ferrite fraction, Equation 2 can not be solved analytically. The fraction ferrite is therefore determined in an iterative process, for which the Newton-Raphson method is used.

In the second part of the transformation only pearlite can be assumed to form. This means that the ferrite fraction,  $f^\alpha$ , is constant. No further austenite enrichment occurs, the austenitic volume is therefore only temperature dependent. The fraction pearlite is then readily found from

$$f^p = \frac{V - V^\gamma + f^\alpha(V^\gamma - V^\alpha)}{V^p - V^\gamma}. \quad (3)$$

The fraction ferrite as found from the analysis of the high-temperature part of the curve determines both the (constant) carbon concentration of the austenite during the pearlite formation and the ratio of cementite and ferrite in the pearlite.

In the case of assumed non-overlapping transformations, the temperature range of the transformation is divided into a temperature range  $T > T_s$ , in which the dilatation is to be analysed as due to ferrite formation, and a temperature range  $T < T_s$ , in which the dilatation is to be analysed as due to pearlite formation. Two assumptions can be made to define  $T_s$ . The first possible assumption is that pro-eutectoid ferrite formation takes place until the final equilibrium fraction ferrite,  $f_{eq}^\alpha$  is obtained. The temperature  $T_s$  then equals the temperature at which  $f^\alpha = f_{eq}^\alpha$ . A second possible criterion to switch from the ferrite analysis to the pearlite analysis is to choose  $T_s$  as the temperature at which the (second) point of inflection occurs in the length change with respect to the temperature. The point of inflection indicates an increased transformation velocity, which is expected at the start of the pearlite formation. (The first inflection point corresponds to the start of the ferrite formation.)

The distinction of temperature ranges for ferrite formation and for pearlite formation is somewhat artificial, but necessary to deduce different phase fractions from a single measurement. Simultaneous formation of ferrite and pearlite in a limited temperature range is in principle possible, but cannot be distinguished by dilatometry. Both methods to determine  $T_s$ , however, have their drawbacks. Using the equilibrium ferrite fraction can easily lead to small errors for two reasons. First, due to higher cooling rates, the ferrite fraction that is actually formed can be different from the equilibrium ferrite fraction. And secondly, small deviations, due to ex-

perimental inaccuracies, in the determined ferrite fraction can lead to relatively large shifts in the pearlite start temperature  $T_s$ . Using the point of inflection in the measured dilatation data to determine  $T_s$  seems more appropriate but is not always possible, especially at high cooling rates.

### 3. Dilatometry

The volume change of a sample can be monitored by means of a dilatometer. The dilatometer measures length changes. For the analysis of the data it is assumed that the expansion/contraction is isotropic. For small relative volume changes the measured length change is related to the volume change by

$$\frac{\Delta L}{L_0} = \frac{1}{3} \frac{\Delta V^s}{V_0^s} = \frac{1}{3} \frac{\Delta V}{V_0}, \quad (4)$$

where  $\Delta L$  is the measured length change,  $L_0 = 10.0$  mm the initial length,  $\Delta V^s$  and  $V_0^s$  the volume change and the starting volume of the sample, and  $\Delta V$  and  $V_0$  the average atomic volume change and the initial average atomic volume, respectively. In order to introduce the measured dilatation  $\Delta L$  in the Equations 2 and 3, the average atomic volume  $V$  can be written as

$$V = \kappa V_0 \left( \frac{3\Delta L}{L_0} + 1 \right), \quad (5)$$

where  $\kappa$ , a scaling factor, ideally equals 1. In practice, however, some non-idealities occur. First, it is possible that there is a contribution from the dilatation measuring system to the measured signal. Another effect that can occur is a net length change of the sample due to effects of transformation plasticity in combination with non-isotropic conditions [17, 18]. To compensate for such effects, in Equation 5 the scaling factor  $\kappa$  is introduced. In the ideal case the ferrite and pearlite volume fractions can be determined using Equations 2 through 5, with  $\kappa = 1$ .

In the non-ideal case of a dilatometric experiment, the scaling factor can be determined by considering the dilatation signal just before (Equations 1 and 5 with  $f^\gamma = 1$ ) and after (Equations 3 and 5 with  $f^\alpha = f_{eq}^\alpha$  and  $f^p = f_{eq}^p$ ) the transformation. Due to the lack of detailed information on the transformation-plasticity effects, the scaling factor is varied linearly between the values found directly before and after the transformation.

The analysis presented here will be compared to the most widely used method to analyse dilatometry data, the lever-rule method. In the latter method the formation of a single phase is assumed, and the length change of the sample is assumed to be proportional to the fraction of this phase. For the application of this method the dilatation from the higher and lower temperature part of the dilatation curve are extrapolated (see Fig. 2). The fraction transformed determined by this method,  $\phi$ , which is the sum of the ferrite and pearlite fractions, is then assumed to be given by the ratio of the observed dilatation to the maximum possible dilatation at each

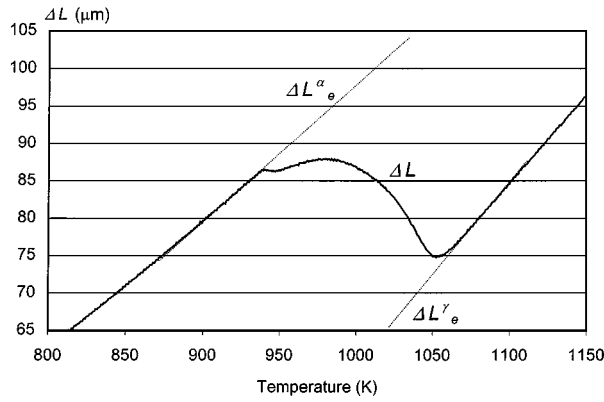


Figure 2 Example dilatation curve during cooling. The straight lines are the extrapolated austenitic length change and the ferritic-pearlitic length change. The fraction transformed according to the lever-rule method ( $\phi$ ) is given by the ratio of the apparent dilatation change,  $\Delta L - \Delta L_e^\gamma$ , to the maximum possible dilatation change,  $\Delta L_e^\alpha - \Delta L_e^\gamma$ .

temperature, and calculated by

$$\phi = \frac{\Delta L - \Delta L_e^\gamma}{\Delta L_e^\alpha - \Delta L_e^\gamma}, \quad (6)$$

where  $\Delta L_e^\gamma$  and  $\Delta L_e^\alpha$  represent the extrapolated dilatations in the high-temperature and low-temperature range respectively.

In using this method two implicit assumptions are made:

- (1) the effect of carbon enrichment of the austenite is negligible, and
- (2) the atomic volumes of ferrite and pearlite are equal.

In order to illustrate the difference between the lever-rule method and the current method, the fractions ferrite obtained by both methods from an artificial dilatation curve have been compared. The dilatation curve is calculated for iron alloyed with 1.0 at.%C (0.22 wt.%C), assuming transformation under equilibrium conditions and using the lattice parameters given in Table I. Fig. 3 shows the results of the analyses of the dilatation curve up to the equilibrium fraction ferrite. For this artificial case, the presently discussed method yields the exact transformation curve. The relative error  $\varepsilon_L$  in the lever-rule results is defined by

$$\varepsilon_L = \frac{\phi - f^\alpha}{f^\alpha}. \quad (7)$$

$\phi$  is the fraction obtained from the lever-rule approach (Equation 6) and  $f^\alpha$  the true fraction ferrite. It can be seen in Fig. 3 that the relative error is largest at the beginning of the transformation, while of course the absolute error (visible as the difference between the two fraction curves) is largest at the end of the ferrite formation. The error is mainly due to neglecting the difference in the ferritic and pearlitic specific volume. In the present method the dilatation signal is related to the specific-volume difference of the austenite phase and the ferrite phase, while in the lever-rule approach an average volume of ferrite and pearlite is used. Since

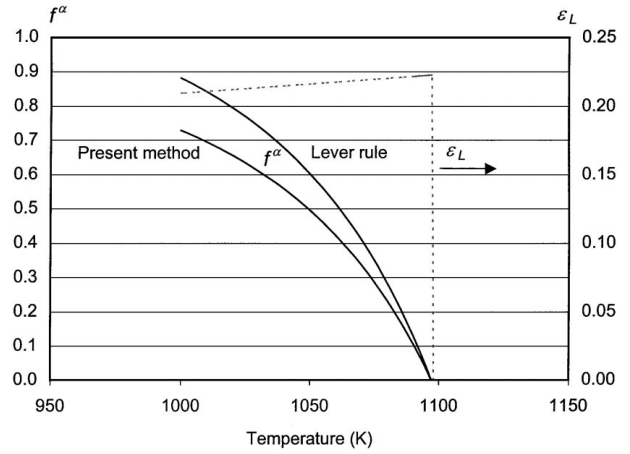


Figure 3 The fractions ferrite determined from a calculated dilatation curve of a steel sample containing 1.0 at.%C by the lever rule and by the presently discussed method, and the resulting relative error,  $\varepsilon_L$ , in the fraction ferrite.

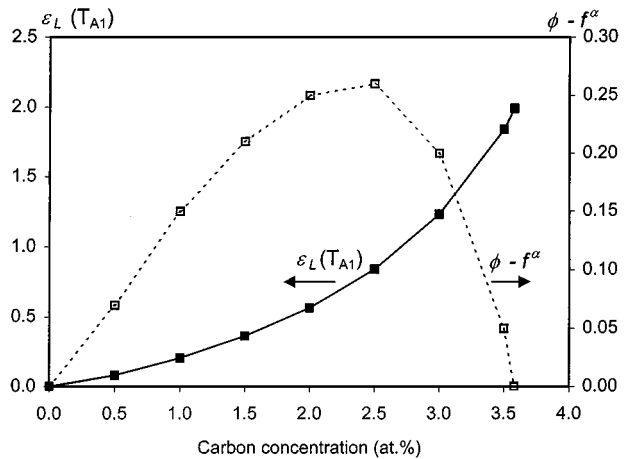


Figure 4 The relative and absolute maximum difference between the fraction ferrite determined by the lever rule and by the present approach at the  $A_1$ -temperature as a function of the carbon concentration.

in reality the pearlitic volume is larger than the ferritic volume, the effect of pearlite formation is underestimated, and therefore the extent of ferrite formation is overestimated. The difference increases with increasing carbon concentration. In the course of the transformation this error is slightly compensated by not taking the enrichment of the austenite into account. Therefore during the transformation there is a slight and continuous decrease in  $\varepsilon_L$ . The analysis of the error connected to the application of the lever rule has been performed for several carbon concentrations. In Fig. 4 the value of  $\varepsilon_L$  at the pearlite-formation temperature  $T_{A1}$  for several alloys with varying carbon concentration is given. It can be seen that there is a progressively increasing relative error,  $\varepsilon_L(T_{A1})$ , with increasing carbon concentration. For higher carbon concentrations less ferrite is formed and therefore the maximum absolute difference,  $\phi - f^\alpha$ , in the determined ferrite fraction diminishes.

For the pearlite formation a similar comparison can be made and the argumentation for the fractions ferrite applies for the pearlite fractions as well. For clarity of the discussion only the results of the comparison of

TABLE II Compositions of the alloys in weight percentages. For carbon the atomic percentages are given as well (in brackets)

alloy	C (at.%)	Mn	Si	Cu	Cr	Ni	Mo	Sn	P	S	N
C05	0.055 (0.26)	0.237	0.008	0.009	0.023	0.024	0	0.002	0.011	0.013	-
C07	0.072 (0.33)	0.365	0.007	0.010	0.024	0.024	0.002	0	0.012	0.013	-
C10	0.103 (0.48)	0.490	0.006	0.009	0.018	0.021	0	0	0.01	0.014	-
C22	0.214 (0.99)	0.513	0.2	0.086	0.021	0.049	0.003	0.003	0.019	0.031	0.007
C35	0.364 (1.67)	0.656	0.305	0.226	0.177	0.092	0.016	0.017	0.014	0.021	0.001
C45	0.468 (2.14)	0.715	0.257	0.231	0.193	0.144	0.017	0.013	0.002	0.031	0.009

the fractions ferrite are given and discussed. It should be noted that in principle the lever rule only gives the amount of transformed austenite and does not give information over individual fractions ferrite and pearlite.

#### 4. Experimental

In order to test the presently proposed method, transformation experiments on a series of steels with different carbon contents have been performed. The composition of the samples is given in Table II. The dilatation of the samples as a function of temperature is determined using a Bähr 805A/D dilatometer. Fig. 5 gives a schematic representation of the instrument. The sample is 10.0 mm long with a diameter of 4.0 or 5.0 mm. Two thermocouples, type S, are spot welded onto the sample, which is clamped between quartz push rods. One thermocouple is used to control the heating power and one serves as a reference to verify the temperature homogeneity. The temperature differences between the two thermocouples remain within 10 K. In the present experiments, each sample is heated by induction to a temperature of 1223 K, austenitised for 5 minutes and subsequently cooled at a rate of 20 K/min.

The temperature of the push rods does not remain constant during the measurement due to thermal conductivity effects from the sample. Due to the small ex-

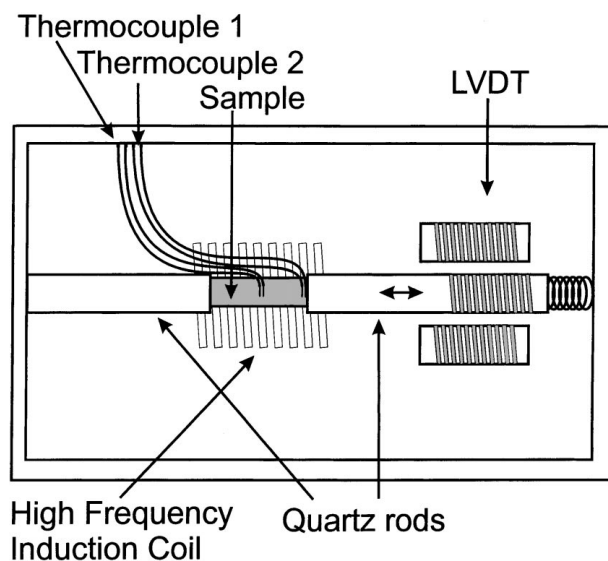


Figure 5 Schematic representation of the dilatometer configuration.

pansion coefficient of quartz,  $0.5 \times 10^{-6} \text{ K}^{-1}$  (the expansion coefficient of steel is approximately  $10 \times 10^{-6} \text{ K}^{-1}$ ), the contribution of the push rods to the measured length is limited. The length change of the sample plus push rods is recorded by a Linear Variable Displacement Transducer.

During the experiment, the heating power is also registered. This provides a means to have an independent absolute temperature reference, since a ferromagnetic material, ferrite at  $T < T_C$  ( $T_C$  is the Curie temperature), is more easily heated by induction than a paramagnetic material, austenite or ferrite at  $T > T_C$ . Therefore, a distinct drop in the power required to keep the sample at the scheduled temperature appears when the sample transforms from the paramagnetic to the ferromagnetic state. The Curie temperature of steel is known to be almost independent of the carbon concentration, but it depends strongly on the manganese concentration. From thermodynamic data it follows that this dependence can be expressed by the relation

$$T_C = 1042 \text{ K} - x_{\text{Mn}} \times 1500 \text{ K}, \quad (8)$$

with  $x_{\text{Mn}}$  the weight fraction manganese.

Fig. 6 gives two examples of such internal temperature checks. The steel C05 contains 0.24 at.% Mn (Table II), which implies that  $T_C = 1038 \text{ K}$ . Steel C10, with more manganese, 0.50 at.%, should have a lower Curie temperature, namely 1034 K. The temperatures

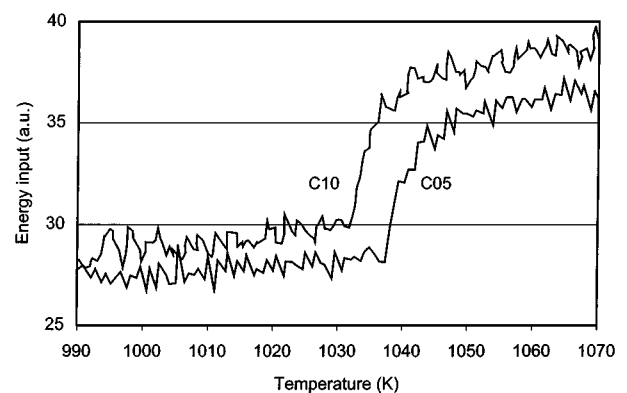


Figure 6 The required power to follow the scheduled temperature programme for the samples C05 and C10. The change in the required power corresponds to the Curie transition.

at which the heating power drops during the measurements indicate that the dilatometer temperature measurement system yields correct absolute temperature values.

## 5. Results and discussion

Fig. 7 depicts the measured dilatation curves, represented as  $\Delta L/L_0$  vs.  $T$ , for the six steel compositions given in Table II. The curves have been shifted along the  $\Delta L/L_0$ -axis in order to make them coincide in the austenite region. It is observed that at higher carbon levels, going from sample C05 to C45, the transformation-start temperature shifts towards lower temperatures. This tendency is readily understood from the phase diagram. Furthermore, it can be seen that the length change caused by the transformation becomes less with increasing carbon content. This was already predicted in the Theory section and is readily understood from Fig. 1. In Fig. 8 the dilatation difference ( $\Delta L - \Delta L_e^Y$ ) at a temperature of 900 K is depicted against the calculated length change at the same temperature. It can

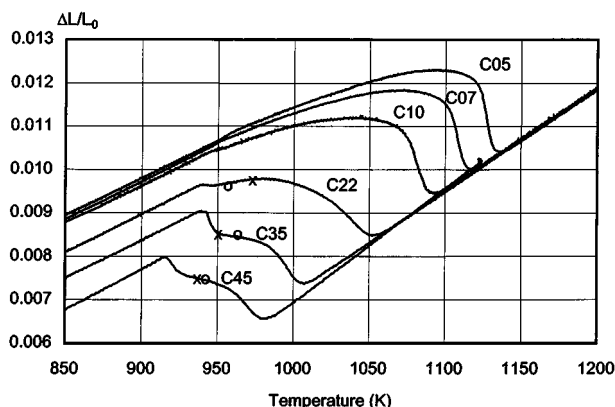


Figure 7 The measured dilatation curves for the six alloys of Table II. The curves are shifted along the  $\Delta L/L_0$ -axis in order to coincide in the austenite region. The crosses and circles indicate the  $T_s$  temperatures, according to the two criteria used.

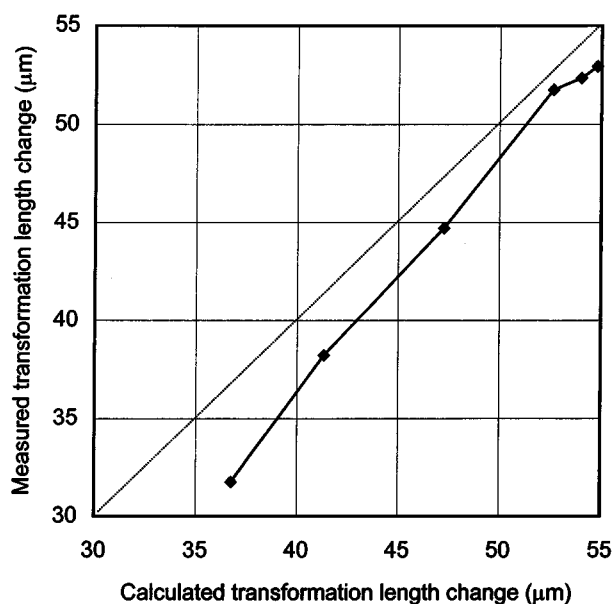


Figure 8 The calculated vs. measured apparent dilatation caused by the transformation for the six compositions determined at 900 K.

TABLE III Experimental scaling factor  $\kappa$  in the ferrite/pearlite and the austenite region

alloy	$\kappa$ in ferrite/pearlite region	$\kappa$ in austenite region
C05	1.0073	1.0078
C07	1.0056	1.0058
C10	1.0037	1.0038
C22	1.0078	1.0075
C35	1.0060	1.0054
C45	1.0046	1.0039

be seen that the measured length change is consistently smaller than the calculated length change. This is consistent with the observation that the length of the sample after a complete transformation cycle is less than at the beginning of the experiment. The most likely explanation of these observations is that they are due to transformation plasticity.

The scaling factor  $\kappa$  (Equation 5) is determined from each measurement as described in the Dilatometry section. The values found for  $\kappa$  are given in Table III. It can be seen that only a slight correction is needed, between 0.4 and 0.8%. The difference between the two  $\kappa$ -values within each measurement never exceeds  $7 \times 10^{-4}$ . Despite the variations being only slight, it is essential to introduce a factor  $\kappa$  to get consistent values for the phase fractions.

In order to deduce the ferrite and pearlite fractions from the dilatation curves the temperature  $T_s$  is chosen, indicating the distinction between the temperature ranges of ferrite and pearlite formation. As previously stated, two approaches are used. In the first approach it is assumed that ferrite is formed until the equilibrium fraction is reached, and that subsequently only pearlite forms. The resulting fractions for the measurements of Fig. 7 are shown in Fig. 9. The transition from ferrite to pearlite is marked with a cross, x, both in Figs 7 and 9. It can be seen that for C05 and C07 there is a temporary decrease in the fraction at the end of the ferrite formation. This is probably due to the application of the linear variation of the scaling factor. As explained before, one of the spurious effects that influences the dilatation curve is transformation plasticity. The plasticity effect is different for the austenite/ferrite transformation and

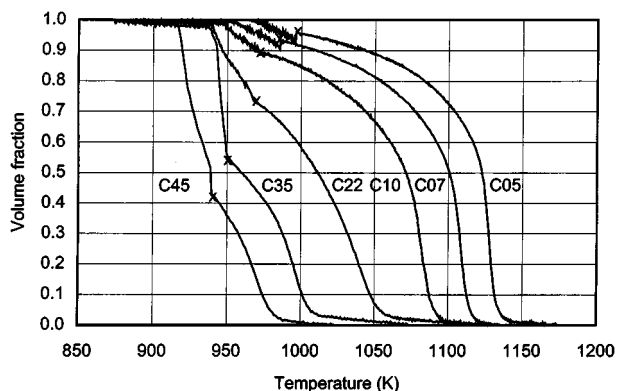


Figure 9 The fraction curves obtained from the present analysis. As the criterion to choose  $T_s$  the equilibrium ferrite fraction was used. The crosses indicate the temperature to switch to the pearlite analysis.

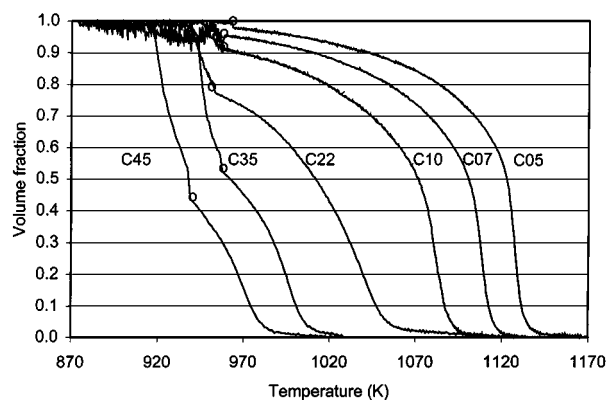


Figure 10 The fraction curves obtained from the present analysis. As the criterion to choose  $T_s$  the point of inflection in the  $L$  vs. temperature plot was used. The circles indicate the temperature to switch to the pearlite analysis.

the austenite/pearlite transformation. Therefore, the linear variation of  $\kappa$  during the complete transformation that is assumed in the analysis, should be seen as a first-order approximation. For low carbon concentrations the difference between the measured volume change and the ferritic volume -the numerator in Equation 2- is small, and therefore very sensitive to the value of  $\kappa$ . The transition temperature  $T_s$  in Fig. 9 coincides well with the temperatures at which an accelerated transformation rate is observed. There is a considerable variation in the pearlite start temperatures of the several materials. This variation in the  $A_{r1}$  temperature seems large in view of the variation in chemical composition of the alloys and their reaction kinetics.

Fig 10 gives the results when using the second approach for the choice of  $T_s$ . Now, the pearlite start temperatures as indicated by the inflection point in the dilatation curve (Fig. 7, marked with an o) are used to switch to the pearlite analysis. Comparing with the results depicted in Fig. 9, the pearlite start temperatures have shifted significantly (see Table IV and Fig. 7), especially for low carbon contents, causing the  $A_{r1}$  temperatures for the six alloys to be within a smaller range. Nevertheless, the deviations in the ferrite fraction between the results for the two different transition criteria are only slight. The unrealistic drop in the fraction curves for lower carbon contents does not appear in Fig. 10. All in all, the choice of using the point of inflection to determine  $T_s$  leads to more consistent transformation curves than determining  $T_s$  through the equilibrium ferrite fraction. Nevertheless, the differences between both approaches are not very large, especially when considering the ferrite formation. This

TABLE IV Pearlite start temperatures as obtained from the criteria "equilibrium fraction ferrite" and "point of inflection" (see text)

alloy	Equilibrium fraction	Point of inflection
C05	996 K	963 K
C07	986 K	958 K
C10	973 K	958 K
C22	967 K	953 K
C35	949 K	956 K
C45	941 K	943 K

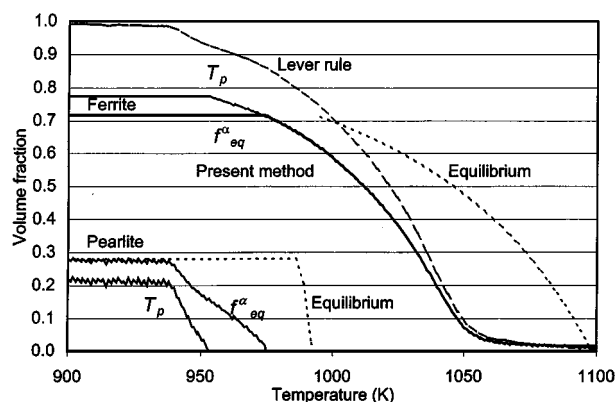


Figure 11 The fraction curves obtained from a measurement by applying the present analysis (solid lines), once with the equilibrium ferrite fraction criterion ( $f_{eq}^{\alpha}$ ) and once with the inflection point criterion ( $T_p$ ). The results from applying the lever rule are represented by the dashed line. Furthermore fraction curves for sample C22 according to equilibrium (short dashed lines) are given.

is of importance when the point of inflection cannot accurately be determined, for instance at high cooling rates. As an illustration, the difference in the transformation curves resulting from the two approaches is shown for C22 in Fig. 11. The ferrite parts of the transformation curves coincide up to the formation of pearlite for the equilibrium-fraction choice. Both the amount of pearlite and the pearlite formation rate are significantly influenced by the criterion for  $T_s$ . Also given in Fig. 11 is the transformation curve resulting from the application of the lever rule to the same experimental data. The error in the transformation curve is considerable. In a small temperature range the calculated fraction even exceeds the calculated equilibrium fraction.

Fig. 11 is an adequate summary of the effects that have been presented in this paper: the discussed method yields an accurate determination of the ferrite and pearlite formation from a dilatometry experiment, where the distinction between ferrite and pearlite formation is only slightly influenced by the criterion for  $T_s$ .

## 6. Conclusion

Dilatometry can effectively be used to obtain data concerning the austenite decomposition of pro-eutectoid steel grades. Both the carbon enrichment of the austenite during the primary ferrite formation and the difference in atomic volume of ferrite and pearlite are quantitatively taken into account. This rigorous approach necessitates a division of the transformation into a ferrite-formation range and a pearlite-formation range. In principle, two different criteria can be used for this choice. It is shown that this choice does not significantly affect the ferrite-formation curve. Significant errors are shown to result from neglecting the carbon enrichment and the difference in ferritic and pearlitic atomic volume.

## Acknowledgements

The financial support from the IOP Metals Programme is gratefully acknowledged. Furthermore we are indebted to Corus Research and Development for the use

of their materials, Marcel Onink, Jeroen Colijn for the stimulating discussions, Nico Geerlofs for assistance with the experiments and Yvonne van Leeuwen for advice concerning the programming.

## References

1. J. W. JOHNSON and R. F. MEHL, *Trans. AIME* **135** (1939) 416.
2. M. AVRAMI, *J. Chem. Phys.* **7** (1939) 1103.
3. *Idem.*, *ibid.* **8** (1940) 212.
4. *Idem.*, *ibid.* **9** (1941) 177.
5. W. T. REYNOLDS, JR., M. ENOMOTO and H. I. AARONSON, in Proc. Conf. Phase Transformations in Ferrous Alloys (Metall. Soc. AIME and ASM, Philadelphia, PA, 1983) p. 155.
6. R. A. VANDERMEER, *Acta Metall. Mater.* **38** (1990) 2461.
7. G. P. KRIELAART, J. SIETSMA and S. VAN DER ZWAAG, *Mater. Sci. Eng.* **A237** (1997) 216.
8. R. F. SPEYER, "Thermal Analysis of Materials" (Marcel Dekker, Inc., New York, 1994).
9. C. GARCÍA DE ANDRÉS, F. B. CABELLERO, C. CAPDEVILA and H. K. D. H. BHADSHIA, *Scr. Mat.* **39** (1998) 791.
10. M. ONINK, F. D. TICHELAAAR, C. M. BRAKMAN, E. J. MITTEMEIJER and S. VAN DER ZWAAG, *Z. Metall.* **87** (1996) 24.
11. M. TAKAHASHI and H. K. D. H. BHADSHIA, *J. Mat. Sci. Lett.* **8** (1989) 477.
12. T. A. KOP, J. SIETSMA and S. VAN DER ZWAAG, in Proceedings from Materials Solutions '97 on Accelerated Cooling/Direct Quenching Steels, 15–18 September 1997, Indianapolis, Indiana (ASM International, Materials Park Ohio, 1997) p. 159.
13. H. STUART and N. RIDLEY, *J.I.S.I.* **204** (1966) 711.
14. M. ONINK, C. M. BRAKMAN, F. D. TICHELAAAR, E. J. MITTEMEIJER, S. VAN DER ZWAAG, J. H. ROOT and N. B. KONYER, *Scr. Metal. Mat.* **29** (1993) 1011.
15. C. QUI and S. VAN DER ZWAAG, *Steel Research* **68** (1997) 32.
16. R. C. REED and J. H. ROOT, *Scr. Mat.* **8** (1998) 95.
17. J. B. LEBLOND, G. MOTTET and J. C. DEVAUX, *J. Mech. Phys. Solids* **34** (1986) 395.
18. R. KENNEDY, A. I. GRANT, A. J. KINNEAR and I. M. KILPATRICK, *J.I.S.I.* **208** (1970) 601.

*Received 8 December 1998  
and accepted 21 June 2000*